Effectiveness of Three Decontamination Treatments against Influenza Virus Applied to Filtering Facepiece Respirators

MICHAEL B. LORE[1], BRIAN K. HEIMBUCH[2], TEANNE L. BROWN[1], JOSEPH D. WANDER[3] and STEVEN H. HINRICHS[1]*

[1]*Department of Pathology and Microbiology, University of Nebraska Medical Center, Omaha, NE 68198, USA;* [2]*Engineering and Science Division, Applied Research Associates, Panama City, FL 32401, USA;* [3]*Airbase Sciences Branch, Air Force Research Laboratory, Tyndall Air Force Base, FL 32403, USA*

Filtering facepiece respirators (FFRs) are recommended for use as precautions against airborne pathogenic microorganisms; however, during pandemics demand for FFRs may far exceed availability. Reuse of FFRs following decontamination has been proposed but few reported studies have addressed the feasibility. Concerns regarding biocidal efficacy, respirator performance post decontamination, decontamination cost, and user safety have impeded adoption of reuse measures. This study examined the effectiveness of three energetic decontamination methods [ultraviolet germicidal irradiation (UVGI), microwave-generated steam, and moist heat] on two National Institute for Occupational Safety and Health-certified N95 FFRs (3M models 1860s and 1870) contaminated with H5N1. An aerosol settling chamber was used to apply virus-laden droplets to FFRs in a method designed to simulate respiratory deposition of droplets onto surfaces. When FFRs were examined post decontamination by viral culture, all three decontamination methods were effective, reducing virus load by >4 log median tissue culture infective dose. Analysis of treated FFRs using a quantitative molecular amplification assay (quantitative real-time polymerase chain reaction) indicated that UVGI decontamination resulted in lower levels of detectable viral RNA than the other two methods. Filter performance was evaluated before and after decontamination using a 1% NaCl aerosol. As all FFRs displayed <5% penetration by 300-nm particles, no profound reduction in filtration performance was caused in the FFRs tested by exposure to virus and subsequent decontamination by the methods used. These findings indicate that, when properly implemented, these methods effectively decontaminate H5N1 on the two FFR models tested and do not drastically affect their filtering function; however, other considerations may influence decisions to reuse FFRs.

Keywords: bioaerosol; decontamination; healthcare workers; influenza virus; N95 respirator; respirator reuse

INTRODUCTION

The recent emergence of novel strains of influenza virus has renewed public health interest in the transmission and control of infectious agents. Significant attention has been placed on the avian influenza

virus H5N1 and 2009 H1N1 (California) influenza virus type A. The communicable nature of these pathogens has created demand for inexpensive and efficient respiratory protection. Disposable filtering facepiece respirators (FFRs) are commonly used to reduce the exposure to airborne particles. FFRs have been recommended for use as part of a comprehensive infection control strategy by the Centers for Disease Control and Prevention (CDC). Manufacturers of respirators [those that are both approved by the

*Author to whom correspondence should be addressed.
Tel: +1-402-559-9415; fax: +1-402-559-7799;
e-mail: mlore@unmc.edu

National Institute for Occupational Safety and Health (NIOSH) as respirators and approved by the Food and Drug Administration (FDA) for medical uses] recommend that they be discarded if soiled or contaminated. However, the epidemic potential of influenza raises concerns that the manufacturing supply of FFRs would be unable to meet a sudden surge in demand. The Institute of Medicine (IOM) estimated that the healthcare sector would require 90 million FFRs for a 6-week influenza pandemic outbreak (Bailar *et al.*, 2006). This estimate, combined with the Occupational Safety and Health Administration's (OSHA) prediction that an influenza pandemic would last 24 weeks (OSHA, 2009), suggests that an outbreak could require as many as 360 million FFRs. The likelihood of widespread FFR shortages has prompted the consideration of re-use of FFRs during pandemics, when supply is short and the device has not been visibly soiled or damaged (Bailar *et al.*, 2006; Siegel *et al.*, 2007; APIC, 2009; OSHA, 2009; CDC, 2010). Although reuse may increase the potential for cross-contamination, FFR shortages may impose a far greater burden on the ability to control an outbreak. Therefore, a need exists for objective experimental information upon which decisions about the safety and practicality of decontamination for reuse of FFRs can be based.

FFRs remove pathogenic microorganisms from aerosols generated by infected individuals and are thus potentially fomites. Viability of influenza virus on inanimate surfaces is well-recognized even though it may be highly variable (Bean *et al.*, 1982; Brady *et al.*, 1990; Tiwari *et al.*, 2006; Boone and Gerba, 2007; Weber and Stilianakis, 2008). Since previously worn FFRs may serve as a reservoir for the spread of virus, the reuse of filters exposed to microorganisms requires careful consideration. If respirator shortages are to be mitigated through reuse, rapid, low-cost, and efficient decontamination methods must be established.

This study evaluated the virucidal capability of three energetic decontamination methods: ultraviolet germicidal irradiation (UVGI), microwave-generated steam (MGS), and moist heat (MH). These methods were utilized to two models of commercially available NIOSH-approved N95 FFRs, on which standardized quantities of influenza (A/H5N1) virus were applied as aerosolized droplets.

METHODS

Experimental design

FFR models 1860s and 1870 (3M Company, St Paul, MN, USA) were selected for study and exposed to in-fluenza virus-containing aerosol using an aerosol test system. Influenza virus type A of the low-pathogenicity H5N1 strain was selected for use. Table 1 shows the study design, whereby a total of 108 FFRs were exposed and studied. 'Exposure' refers to the application of virus and 'treatment' refers to application of any one of the three decontamination procedures. The treated respirators were subjected to one of three decontamination methods while the non-treated respirators served as controls and were exposed to virus but received no disinfection treatment. All untreated FFRs were incubated for the same duration of time and at the same environmental conditions (temperature and humidity) as the treated respirators.

Treatment and extraction times were held constant between FFRs exposed to virus and the controls. Virus was applied using the droplet method described below.

Respirator descriptions. Two models of N95 FFRs common in healthcare settings were chosen for this study: 3M models 1860s (small size)—a ridged, cup-shaped design—and 1870, a flat-fold/three-panel design. Both designs are multi-layered and use a filtration medium of electrostatically charged, polypropylene microfibers. These FFRs are commercially available and carry a NIOSH N95 filter efficiency rating (NIOSH Federal Respiratory Regulations 42 CFR Part 84). The N95 designation certifies that respirators are ≥95% efficient at capturing oil-free airborne particles and aerosols with an aerodynamic mass median diameter of 300 nm when evaluated at the NIOSH-specified test conditions. These respirators have also been approved by FDA as medical devices.

Virus stock. Influenza A/H5N1 (VNH5N1) was acquired from the CDC and transferred with authorization to a commercial laboratory for production in eggs. Virus was produced and recovered from allantoic fluid and quantified. After receipt, the virus stock was re-titered in house. The viral titer was $\sim 5.5 \log_{10}$ median tissue culture infective dose assay (TCID-50) ml-1_{50} ml^{-1}.

Droplet chamber. The aerosol test system (Fig. 1) used in this study was designed to mimic respiratory droplet transmission of viruses onto surfaces (ASTM: E2721-10, ASTM, 2010). The chamber was composed of a stainless steel box measuring

Table 1. FFR sample sets exposed to H5N1 virus.

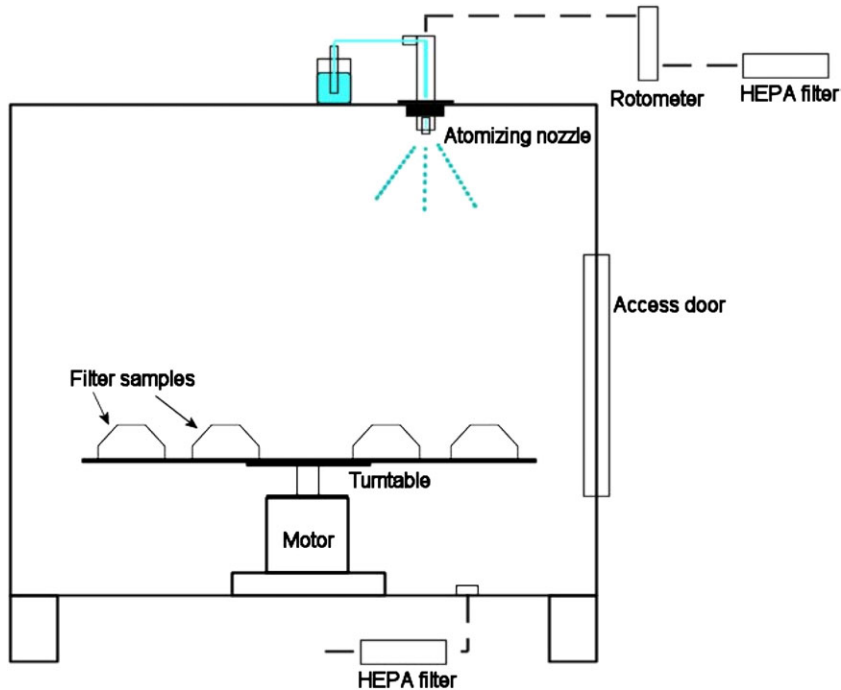| FFR models	Control	UVGI	Control	MGS	Control	MH	# Tests
3M 1860s	9	9	9	9	9	9	54
3M 1870	9	9	9	9	9	9	54
				Total			108

Fig. 1. Schematic of the aerosol test system.

$61 \times 61 \times 76$ cm with an approximate volume of 283 l. A pneumatic atomizing nozzle mounted vertically in the top of the chamber generated large, virus-laden droplets as described below. Airflow inside the chamber was designed to allow direct settling onto the FFRs. FFRs were rotated slowly on a turntable inside the chamber to achieve uniform deposition. Air containing excess aerosol flowed out of the chamber through a high efficiency particulate air (HEPA) filter at the bottom. Relative humidity (RH) and temperature within the test chamber were measured and maintained at constant levels throughout the testing. The aerosol test chamber was operated within a BSL3 laboratory facility and housed inside a Purair 20 ductless fume hood (Air Science LLC, Fort Myers, FL, USA).

Droplet size characterization. Droplet size distribution of the nozzle was characterized using a Spraytec droplet analyzer (Malvern, Worcestershire, UK) using standard conditions specified by the manufacturer. The Spraytec could not be directly linked with the chamber so the nozzle was analyzed external to the chamber, which may have produced smaller droplets due to an overall reduction in RH. The nozzle was operated at the same conditions used in this study (see below) and droplets were analyzed at five locations downstream of the nozzle (5, 15, 30, 45, and 60 cm).

Viral droplet loading protocol. Respirators were arranged in two equally spaced, concentric circles on the rotating platform inside the aerosol chamber. The door was sealed and rotation of the platform was adjusted to three revolutions per minute. As the table revolved, the pneumatic atomizing nozzle (model 2000VL; Paasche, Chicago, IL, USA) delivered 25 ml of influenza A/H5N1 virus suspension at a concentration of 5.5 $\log_{10}$ TCID$_{50}$ ml^{-1}.

A flowmeter (Cole–Parmer, Vernon Hills, IL, USA) regulated delivery of $\sim$4 l min^{-1} of HEPA-filtered air to the nebulizer, which atomized $\sim$5 ml of viral suspension per minute until the reservoir was depleted. The average time of exposure ranged between 5 and 8 min. After exposure, the airflow was shut off and aerosol remaining within the chamber was allowed to settle for 3 min before the respirators were removed. Treated filters were exposed to one of the three decontamination methods while the non-treated filters were used as controls. All aerosol tests were conducted using an undiluted virus concentration of 5.5 $\log_{10}$ TCID$_{50}$ ml^{-1}. Under test conditions, the RH within the chamber was $>$60% and the temperature range was 22 ± 2°C.

Virus extraction efficiency. To determine the extraction efficiency from the test material, a single circular coupon was cut from each of the four quadrants of the FFRs using a 3.8-cm diameter (11.3 cm^2) arch

punch (C.S. Osborne & Co., Harrison, NJ, USA). A volume of 250 µl of virus stock (1 ml total per set) was pipetted onto each coupon and allowed to dry for 20 min inside the biosafety cabinet. The coupons (four total) were placed in a 50-ml conical tube containing 15 ml of serum-free Eagle's minimum essential medium (sf-EMEM) supplemented with 1% penicillin–streptomycin and 10% L-glutamine. Conical tubes were mixed for 20 min to liberate virus particles from the coupons using a multi-tube vortex mixer (VWR Scientific, West Chester, PA, USA) at maximum speed. The supernatants were then removed from the tubes and aliquots assayed for viable virus particles through log serial dilutions in sf-EMEM. Results were expressed as virus titers in units of $\log_{10}$ TCID$_{50}$ ml^{-1}. Quantitative real-time polymerase chain reaction (qRT-PCR) was performed on the recovered supernatant and mean cycle threshold (Ct) values were compared to the stock concentration. Each experiment was performed in triplicate.

Virus culture quantification. Virus was quantified using Diagnostic HYBRIDS FreshCells™ cell cultures (Athens, OH, USA). The Madin–Darby canine kidney cells were maintained using standard methods, plates were incubated, and wells were monitored daily for presence or absence of cytopathic effect (CPE) by observation with an inverted light microscope. On day five, adherent cells were fixed with 400 µl of a 0.07% (w/v) crystal violet and 10% (v/v) glutaraldehyde solution for 1 h. Plate-well monolayers were scored for CPE and virus titers

quantified according to the Spearman–Karber formula (Finney, 1978). The cell culture limit of detection was empirically set at >0.5 $\log_{10}$ TCID$_{50}$. Therefore, any data resulting in values below the detection limit (BDL) were expressed as zero in log reduction calculations (Tables 2 and 3).

Decontamination procedures. Virus-laden respirators were subjected to one of three decontamination procedures as described below. The orientation of the filter was convex panel facing the droplet or treatment source. Controls were subjected to the same decontamination procedures as the treated FFRs but were not exposed to virus.

Ultraviolet germicidal irradiation. A 126- (L) × 15.2- (W) × 10.8-cm (H), dual-bulb, 15-W UV-C (254-nm wavelength) lamp (Ultraviolet Products, Upland, CA, USA) was placed in a Labgard class II, type A2, laminar flow cabinet (NuAire, Inc., Plymouth, MN, USA) set to a height 25 cm above the cabinet's working surface. Measured by a UVX digital radiometer (UVP Inc., Upland, CA, USA), the lamp's UV-C wavelength irradiance ranged between 1.6 mW cm^{-2} and 2.2 mW cm^{-2}. Virus-laden respirators were placed inside the cabinet, directly under the ultraviolet lamp with the convex panel facing the treatment, and exposed for a total of 15 min at a UV-C wavelength dose of 18 kJ m^{-2}.

Microwave-generated steam. A 1250-W (2450 MHz) commercially available microwave oven (Panasonic Corp., Secaucus, NJ, USA) with a rotating glass plate was used to irradiate a single respirator per treatment. Samples were placed above

Table 2. Mean $\log_{10}$ TCID$_{50}$ virus concentrations recovered from 3M 1860s FFRs.

3M 1860s	UVGI		MGS		MH	
	Non-treated	Treated	Non-treated	Treated	Non-treated	Treated
Replicate 1	4.51	BDL[a]	4.76	BDL[a]	4.68	BDL[a]
Replicate 2	4.68	BDL[a]	4.84	BDL[a]	4.68	BDL[a]
Replicate 3	4.43	BDL[a]	4.84	BDL[a]	4.51	BDL[a]
ΔLog$_{10}$ TCID$_{50}$	>4.54		>4.81		>4.62	

Non-treated, No decontamination procedure was performed (control group).
[a]BDL < 0.5 $\log_{10}$ TCID$_{50}$.

Table 3. Mean $\log_{10}$ TCID$_{50}$ virus concentrations recovered from 3M 1870 FFRs.

3M 1870	UVGI		MGS		MH	
	Non-treated	Treated	Non-treated	Treated	Non-treated	Treated
Replicate 1	4.93	BDL[a]	4.76	BDL[a]	4.68	BDL[a]
Replicate 2	4.68	BDL[a]	4.76	BDL[a]	4.68	BDL[a]
Replicate 3	4.34	BDL[a]	4.84	BDL[a]	4.59	BDL[a]
ΔLog$_{10}$ TCID$_{50}$	>4.65		>4.79		>4.65	

[a]BDL < 0.5 $\log_{10}$ TCID$_{50}$.

a plastic box filled with 50 ml of room temperature tap water. The top of the box was perforated with 96 holes (7 mm diameter) evenly distributed over the entire surface to allow MGS to vent through the respirator. The virus-contaminated respirator was placed with the convex surface pointed toward the steam source and the FFR was then irradiated for 2 min at full power.

Moist heat. A 6-l sealable container (19 × 19 × 17 cm) was filled with 1 l of tap water, placed in an oven (Thermo Fisher Scientific Inc., Marietta, OH, USA), and heated to 65 ± 5°C for 3 h. This allowed the liquid to reach the desired temperature prior to any decontamination tests. For testing, the container was removed from the oven and a single virus-contaminated respirator was placed on the rack. For each decontamination procedure, the container was opened and the FFR placed onto the rack with the convex surface pointed toward the water layer. The container was then sealed and returned to the oven for the 20-min treatment.

Physical penetration measurements. To determine whether the decontamination methods had any effect on the filter performance, each of the three decontamination methods described above was applied to five separate samples of each model of FFR listed in Table 1. Physical penetration measurements were then conducted with a 1% NaCl aerosol challenge as described in Lore *et al.* (2010). Filter testing was performed at a flow rate of 85 l min^{-1}, the flow rate specified by NIOSH for FFR certification testing.

Data analysis

Determination of viable virus concentrations. Viable virus particles were quantified by median TCID$_{50}$ using the Spearman–Karber formula (Finney, 1978). This widely used methodology utilizes dilutions of pathogenic agents to demonstrate absolute thresholds of infectivity (0 or 100%). Infectivity is defined as the concentration capable of producing an observable CPE in the cell culture monolayer. Sample inocula were performed over a range of geometric series dilutions that bracketed the infectivity threshold. This allowed for positive identification of infectivity and proper application of the Spearman–Karber formula. The $\Delta\log_{10}$ TCID$_{50}$ between the control samples and the treated samples was calculated as $\Delta\log_{10}$ TCID$_{50}$ = $\log_{10}$ TCID$_{50}$ (control) − $\log_{10}$ TCID$_{50}$ (test). Results were expressed as virus titers in units of $\log_{10}$ TCID$_{50}$ ml^{-1}.

Virus quantification by qRT-PCR. Viral RNA (vRNA) was extracted using a QIAamp vRNA extraction kit (Qiagen, Hilden, Germany) according to the manufacturer's instructions. The vRNA was recovered in 15 µl (final volume) of elution buffer and quantitated spectrophotometrically (in triplicate) using NanoDrop ND-1000 (Saveen Werner, Limhamn, Sweden). vRNA amplification of the hemagglutinin viral protein target (H5a) was carried out according to the CDC protocol using Invitrogen's SuperScript III Platinum One-Step qRT-PCR System (cat no. 11732-088), which combines the reverse transcription and amplification steps.

Assay conditions for quantification of extracted vRNA were optimized in a Roche LightCycler 480 Real-Time PCR System (Roche Diagnostics). The Superscript III Platinum mastermix reaction components were prepared to the indicated end concentration: 5.5 µl nuclease-free water, 0.5 µl H5a-F forward primer (SO3307; CDC), 0.5 µl H5a-R reverse primer (SO3308; CDC), 0.5 µl H5a-P probe (SO3294; CDC), SuperScript III RT/Platinum *Taq* mix (Invitrogen), and 12.5 µl ×2 PCR master mix. For each sample, 20 µl of the complete LightCycler mastermix and 5 µl of extracted vRNA (25 µl total) were loaded into each well of a 96-well plate. The plate was then loaded into the LightCycler. Samples were run in triplicate for each dilution and presented as the Ct value.

The qRT-PCR thermocycling parameters were as follows: initial complementary DNA synthesis at 50°C for 30 min and then denaturation at 95°C for 2 min, followed by 45 cycles of 15 s of denaturing at 95°C, 30 s of annealing at 55°C, and 30 s of extension at 72°C with a final holding step at 4°C. Total run time was ∼2 h. The cut-off for determining a negative sample was 37 Ct units.

A standard curve was generated from a dilution series constructed from an extracted stock virus sample. RT-PCR was performed on serial log dilutions of the stock in triplicate using the Roche LightCycler 480. These data provided the reference standard by which experimental samples could be extrapolated. Efficiency of the RT-PCR reaction was estimated through linear regression analysis of the dilution curve. This was performed using the LINEST function of Microsoft Excel v2007 (Microsoft Corporation, Redmond, WA, USA), which draws the best-fit line using the least-squares method of regression analysis.

The limit of quantification (LoQ) was determined for the qRT-PCR reaction by serial log dilution of extracted vRNA to the lowest dilutions reliably detectable (−7 and −8). Twenty replicate series of both dilutions were prepared and run simultaneously in triplicate. A confidence interval (CI) was then calculated by multiplying the non-amplified samples by 5 and subtracting from 100. This number was then reported as a percentage. Only threshold cycle values

<40 were included in the data set. A CI of $\geq 95\%$ was utilized. Sample dilutions with Ct values above 36.5 were considered negative.

RESULTS

The consideration for reuse of FFRs following decontamination must address two major issues: first, whether the FFR retains full function and provides a similar level of protection after treatment and second whether the decontamination treatment is effective at reducing the infectious capability of the targeted organism. This study focused primarily on the second point and the development of methods for accurate assessment of the amount of virus contaminating the FFR and the amount removed by the decontamination method. To achieve this goal, the first challenge was to demonstrate uniform application of virus-laden droplets and recovery of virus from FFRs.

Droplet size variation

Droplets at the source were 5 μm count median diameter (CDM) and they grew to ∼12 μm CMD at the 30-cm mark, presumably due to coalescence of the droplets. The droplet size at the 60-cm mark was back down to 5 μm again, which is most likely due to evaporation.

Virus recovery and extraction efficiency

FFRs are intended to protect the user by capturing infectious particles within the composite materials of the device, either the surface covering or the filtering medium. Due to uncertainty about the depth to which virus would penetrate the cover web, all layers were sampled. Following application of virus to the FFRs, a total of four, circular, full-thickness cuttings (coupons) were taken comprising a total area of 45.36 cm^2. Because this study focused on vertical settling of large droplets, only the panel facing the droplet source was sampled. The total estimated area of the convex surface of 1860s and 1870 was 129.46 and 202.79 cm^2, respectively. The efficiency of recovery of vRNA from all coupon replicate sets was $70 \pm 5\%$ (data not shown) as determined by qRT-PCR.

qRT-PCR limit of detection, LoQ, and calibration

The limit of detection of the PCR method was determined as summarized in the methods section using serial dilutions of vRNA. Using a CI limit of 95%, the Roche LightCycler 480 reliably detected a 7-log serial dilution of the H5N1 virus stock. The slope of the standard curve used for calibration purposes was -3.48 with an R^2 value of 0.998.

Decontamination assessed by viral culture

The effect of the three decontamination treatments was assessed on two different models of FFRs (Table 1). Viral recovery from FFRs with and without treatment was assessed by the tissue culture method. Results comparing the recovery of virus expressed as $\log_{10} TCID_{50}$ ml^{-1} are shown in Tables 2 and 3 for 1860s and 1870 respirators, respectively. Each value reported within the table was the mean of three FFRs tested under identical conditions. In total, 27 treated and 27 untreated FFRs were tested for each model of FFR. The decrease in virus titer was calculated by subtracting the average of the treated group from the untreated (control) group. Results were reported as the mean log reduction in virus titer. In all cases, decontamination procedures resulted in viable counts below the cell culture assay's detection limit (BDL).

The mean concentration of influenza A/H5N1 virus recovered from all untreated (control) 1860s samples was 4.66 $\log_{10} TCID_{50}$. Within each treatment, the virus titer replicates were within ± 0.25 SD $\log_{10} TCID_{50}$ of each other and between groups ± 0.27 SD $\log_{10} TCID_{50}$ (Table 2).

The mean concentration of influenza A/H5N1 virus recovered from all untreated (control) 1870 samples was 4.70 $\log_{10} TCID_{50}$. Within each treatment group, the virus titer replicates were within ± 0.59 $\log_{10} TCID_{50}$ of each other and between groups ± 0.14 $\log_{10} TCID_{50}$ (Table 3).

The average log recovery of virus obtained for all untreated controls with the 1860s was 4.66 $\log_{10} TCID_{50}$, similar to the 3M 1870, from which recovery was 4.70 $\log_{10} TCID_{50}$. The $\log_{10} TCID_{50}$ reduction for the decontaminated 1860s respirators was ≥ 4.54 (UVGI), ≥ 4.81 (MGS), and ≥ 4.62 (MH). The $\log_{10} TCID_{50}$ reduction for the 1870 respirators exposed to decontamination methods was ≥ 4.65 (UVGI), ≥ 4.79 (MGS), and ≥ 4.65 (MH). All three decontamination methods achieved an absolute log reduction of >4.0 logs for both respirator models.

Decontamination assessed by qRT-PCR

vRNA extraction was performed on an aliquot of the same eluate used to recover viable virus, and qRT-PCR was performed as described. All values are reported as Ct units representing the number of amplification cycles. Testing of the coupons from non-treated FFRs (control) showed an average Ct value of 16.72 ± 0.7, demonstrating the reproducibility of the application and recovery process over multiple days. Within-run coefficient of variation was <7%.

Each value within the table represented a mean of nine replicates. Analysis of the treated samples showed a difference in Ct cycles between the UVGI decontamination method and the other two methods, MGS and MH, for both FFR models. Material recovered from UVGI-treated samples required more amplification cycles to detect vRNA than from either of the other methods. Consistent with the $TCID_{50}$ determinations, there was no significant difference between MGS and MH as determined by qRT-PCR (Table 4). These results demonstrated that although no viable virus was detectable following decontamination as measured by culture, none of the methods disrupted the viral genome to a level that could not be amplified by PCR.

Post-decontamination filter performance

Results indicate that the mean penetration at 300 nm was <5% for all FFR models tested (Table 5). These data demonstrate that the decontamination methods did not significantly degrade the filter performance at 300-nm particle size.

DISCUSSION

During pandemics, shortages of FFRs may lead to their reuse to extend supplies. This is currently a potential strategy being considered by several government agencies (e.g. CDC) during times of shortage—provided the respirator is not visibly soiled or damaged and does not impede breathing. However, bioaerosol contamination, which often does not display gross soiling, may pose a risk to the user if viable pathogenic microorganisms are still present. Furthermore, without

Table 4. qRT-PCR Ct and coefficient of variation (CV) values of FFRs exposed to H5N1 aerosol.

	UVGI		MGS		MH	
Ct	Ct	CV (%)	Ct	CV (%)	Ct	CV (%)
3M 1860s						
Control	16.39	4.42	16.14	6.63	16.88	2.71
Treated	30.67	2.97	21.8	5.87	22.98	5.62
3M 1870						
Control	16.59	1.67	16.98	5.66	17.36	3.95
Treated	29.1	5.60	19.81	4.01	20.05	2.45

Table 5. Mean penetration ($n = 5$) of 1% NaCl aerosol at 300-nm particle size.

FFR	Control	UVGI	MGS	MH
1860s (%)	1.08	0.99	1.51	1.04
1870 (%)	0.39	0.37	0.99	0.99

proper guidance and procedures, any non-standardized decontamination method may prove to be inadequate. The functionality of the device must also be considered, as decontamination methods may damage straps, nosefoam, and other components that affect the fit.

The objective of this study was to evaluate the virucidal effects of three energetic decontamination methods—UVGI, MGS, and MH—on FFRs exposed to large droplets delivered as aerosols containing influenza A/H5N1 virus. The viral load deposition in this study represented a 'worst-case scenario', in which the viral load onto the FFRs was in probable excess of what a user in a healthcare setting would realistically expect to encounter. These methods were selected based on several factors including common availability, low cost of the technology, and ease of use. For example, high-energy irradiation is present in many hospitals but would not be available to the general public. Efficacy guidelines have yet to be established for FFR fomite decontamination and pathogenic viruses. However, recommendations have been issued by the IOM regarding reusability of face masks during an influenza pandemic. The IOM suggests that any decontamination method applied to an N95 FFR must eliminate the viral threat, be harmless to the user, and have no deleterious effects on filter performance (Bailar *et al.*, 2006). This recommendation is in agreement with previously published guidance on the virucidal test effectiveness on inanimate surfaces set forth by the Environmental Protection Agency (EPA) (EPA, 1982). Therefore, this study used the EPA criterion of complete inactivation of the virus at all dilutions, quantified using the Spearman–Karber method expressed as $\log_{10} TCID_{50}$, to demonstrate successful decontamination.

In addition to $TCID_{50}$ assays, a molecular-based analysis of the samples was performed using qRT-PCR. This non-culture technique, which detects vRNA with sensitivity several orders of magnitude greater than culture assays, can provide additional insight into the extent of biocidal effects beyond infectivity assays. However, molecular amplification assays for the assessment of decontamination effectiveness have not been addressed by regulatory agencies.

UVGI is a highly energetic short-wave (254 nm) ultraviolet light shown to be a useful sterilization technique in a variety of applications. The virucidal mechanism of UVGI is derived from the energy contained within the electromagnetic wave. Single-stranded RNA viruses have been shown to be especially susceptible to this type of radiation (Rauth, 1965; Tseng and Li, 2005). Miller and Plagemann (1974) demonstrated these effects on mengovirus, an RNA virus analogous to influenza virus. Their results demonstrated

progressively increasing changes in the viral proteins, which are the determinants of infectivity.

In this study, a 15-min exposure to high-intensity UVGI was found to be an effective virucidal treatment.

A reduction of $>4 \log_{10} TCID_{50} ml^{-1}$ was observed for both FFRs, indicating functionally complete removal of detectable virus by culture assay. In comparison, results of the qRT-PCR assay indicated a significant reduction in amplified RNA ($\sim$14 cycles, Table 4) following decontamination procedures; however, amplifiable vRNA remained. These results suggest that the energy input of the UV-GI decontamination method was capable of eliminating viral infectivity as seen by the cell culture (TCID) assay. Our data indicate that the virus' infectivity is destroyed but its RNA genetic signature remains, as shown by the reduction in viral genome amplified. These data are in good agreement with previous observations of the effectiveness of UVGI on FFRs as measured by plaque assay made by Vo *et al.* (2009) and Fisher and Shaffer (2011) using surrogate viruses.

Microwave radiation is a form of radio frequency energy that, as when used in household ovens (2450 MHz), excites water molecules, generating heat. Microwave heating has been shown to inactivate or reduce several species of pathogenic microorganisms (Woo *et al.*, 2000). Despite many well-documented studies on microbial damage by microwave irradiation, the mechanism of action is not entirely understood. However, the presence of moisture appears to be a key factor influencing the biocidal effect (Vela and Wu, 1979; Jeng *et al.*, 1987). Therefore, the combined mechanisms of radiation and steam heat were applied in this study (MGS) where the FFRs were supported above a water reservoir during the decontamination process. This allowed steam generated from the water to pass through the FFR, further enhancing the biocidal effects of the microwave radiation treatment.

The MGS decontamination procedure relied solely on steam for disinfection. The biocidal action of steam is believed to be derived from the liquid phase's latent heat of vaporization, which is released upon contact, allowing the exotherm to denature enzymes and other essential cell constituents of the organism. The MH decontamination method is mechanistically analogous to the MGS decontamination, in which warm moisture acts as the main component of biocidal action. This method was chosen over dry heat sterilization because MH is more effective than dry heat for killing microorganisms and lower heat input is less likely to have deleterious results on filter performance (Hutten, 2007; Viscusi *et al.*, 2007, 2009).

As tested, each method (MGS and MH) was fully effective in inactivating influenza A/H5N1 virus particles for both FFR models. The EPA criterion for virucidal test effectiveness was met in this study, using the virus culture method, by the demonstration of results below detectable limits. Although the virus was completely inactivated by the MGS and MH treatments as assessed by culture methods, qRT-PCR methods were able to detect viral genomic material. More of the viral genomic material remained amplifiable following MGS and MH than after the UVGI treatment (Table 4). This was expected given that the mode of action of both methods is denaturation of proteins. Some vRNA was also denatured, which accounted for the reduction in amplified RNA. The results from treatment by MGS or MH were comparable even though the time of treatment differed from 2 to 20 min, respectively.

One challenge related to decontamination using a microwave-based method is the concern that the metal noseband of FFRs would generate combustion. Previous studies have demonstrated that dry microwave irradiation caused the filtration medium around metallic nosebands to melt (Viscusi *et al.*, 2007, 2009). In this study, the microwave-based decontamination method used steam as the dominant biocidal mechanism. Much of the energy is absorbed by water—reducing the potential for damage to the filtration medium. Gross observation of the FFRs post-MGS treatment showed no signs of filter damage. Furthermore, results of the penetration tests indicated that the decontamination methods did not significantly alter the filter performance at the 300-nm particle diameter (Table 5). It is important to note that, although the physical penetration was measured under conditions similar to those of the NIOSH certification test, these results are not equivalent to official NIOSH certification testing. The filtration measurements reported herein should not be interpreted as having any bearing on whether a particular FFR sample meets its designated NIOSH certification.

Any factor that contributes to nonuniform distribution of steam across the face of the respirator can alter its effectiveness. For MGS, the reservoir's surface area, liquid volume, and microwave power level are significant in relation to the exposure time. Smaller liquid surface areas, larger liquid volumes, or a microwave delivering <1250 W will require longer exposure times to generate sufficient amounts of steam. This decontamination method was the least time intensive and utilized commonly available items found in most households. The low throughput might restrict its use in large healthcare settings but this technology

would be practicable for home use or small organizations. This study was limited to evaluating the effect of three decontamination methods on the mask surface and did not examine the straps or nose clip. Additional evaluation must be considered regarding other components of the FFR prior to general adoption of these decontamination methods. Further research is appropriate to standardize this process and confirm its effectiveness for use by healthcare workers, first responders, and the general public.

CONCLUSION

This study showed that three decontamination methods (ultraviolet germicidal irradiation, MGS, and MH) satisfactorily decontaminated the 3M 1860s and 1870 FFRs as measured by a virus culture method. Within the constraints of the experiment, the three methods were all completely effective for the decontamination of FFRs as assessed by a culture method. These conclusions are further supported by data reported by Heimbuch *et al.* (2011) in which H1N1 droplets and droplet nuclei applied to six models of FFRs were decontaminated using the same three energetic methods described here. The construction or type of FFR did not result in any measured difference among the decontamination methods applied.

These findings suggest that, when properly implemented, these decontamination methods could suppress cross-contamination through contact with FFRs during situations in which reusing FFRs is necessary. However, these conclusions apply only to the models tested in this study—other FFR models may show different effects. Although this study did not investigate the effect of these treatments on fit, Viscusi *et al.* (2011) reported no significant decrease in the protective capability of FFRs following decontamination.

REFERENCES

ASTM. (2010) ASTM International: E2721-10. Standard test method of evaluation of the effectiveness of decontamination procedures for surfaces when challenged with droplets containing human pathogenic viruses. West Conshohocken, PA: ASTM International.

APIC. (2009) Reuse of respiratory protection in prevention and control of epidemic- and pandemic-prone acute respiratory diseases (ARD) in healthcare. [serial online] 2009 http://www.apic.org/Content/NavigationMenu/GovernmentAdvocacy/PublicPolicyLibrary/Reuse_of_Respiratory_Proctection_archive_1209.pdf. Accessed 16 July 2011.

Bailar JC, Brosseau LQ, Cohen HJ, *et al.* (2006) Reusability of facemasks during an influenza pandemic: facing the flu. Washington, DC: National Academies Press.

Bean B, Moore BM, Sterner B *et al.* (1982) Survival of influenza viruses on environmental surfaces. J Infect Dis; 146: 47–51.

Boone SA, Gerba CP. (2007) Significance of fomites in the spread of respiratory and enteric viral disease. Appl Environ Microbiol; 73: 1687–96.

Brady MT, Evans J, Cuartas J. (1990) Survival and disinfection of parainfluenza viruses on environmental surfaces. Am J Infect Control; 18: 18–23.

CDC. (2010) Questions and answers regarding respiratory protection for preventing 2009 H1N1 influenza among healthcare personnel. [serial online] 2010 Available at http://www.cdc.gov/h1n1flu/guidelines_infection_control_qa.htm. Accessed 16 July 2011.

EPA. (1982) Pesticide assessment guidelines. Subdivision G: product performance, Section 91-30. Washington, DC: Environmental Protection Agency. pp. 72–6.

Finney DJ. (1978) Statistical method in biological assay. London, UK: Griffin.

Fisher EM, Shaffer RE. (2011) A method to determine the available UV-C dose for the decontamination of filtering facepiece respirators. J Appl Microbiol; 110: 287–95.

Heimbuch BK, Wallace WH, Kinney K *et al.* (2011) A pandemic influenza preparedness study: use of energetic methods to decontaminate filtering facepiece respirators contaminated with H1N1 aerosols and droplets. Am J Infect Control; 39: 1–9.

Hutten IM. (2007) Handbook of nonwoven filter media. Oxford, UK: Butterworth-Heinemann.

Jeng DK, Kaczmarek KA, Woodworth AG, *et al.* (1987) Mechanism of microwave sterilization in the dry state. Appl Environ Microbiol; 53: 2133–7.

Lore M, Sambol A, Japuntich D, *et al.* (2010) Inter-laboratory performance between two nanoparticle air filtration systems using scanning mobility particle analyzers. J Nanopart Res; 13: 1581–91.

Miller RL, Plagemann PG. (1974) Effect of ultraviolet light on mengovirus: formation of uracil dimers, instability and degradation of capsid, and covalent linkage of protein to viral RNA. J Virol; 13: 729–39.

OSHA. (2009) Pandemic influenza preparedness and response guidance for healthcare workers and healthcare employers. [serial online] 2009. Available at http://www.osha.gov/Publications/OSHA_pandemic_health.pdf. Accessed 16 July 2011.

Rauth AM. (1965) The physical state of viral nucleic acid and the sensitivity of viruses to ultraviolet light. Biophys J; 5: 257–73.

Siegel JD, Rhinehart E, Jackson M *et al.* (2007) 2007 guideline for isolation precautions: preventing transmission of infectious agents in health care settings. Am J Infect Control; 35: S65–164.

Tiwari A, Patnayak DP, Chander Y, *et al.* (2006) Survival of two avian respiratory viruses on porous and nonporous surfaces. Avian Dis; 50: 284–7.

Tseng C-C, Li C-S. (2005) Inactivation of virus-containing aerosols by ultraviolet germicidal irradiation. Aerosol Sci Technol; 39: 1136–42.

Vela GR, Wu JF. (1979) Mechanism of lethal action of 2,450-MHz radiation on microorganisms. Appl Environ Microbiol; 37: 550–3.

Viscusi D, King W, Shaffer R. (2007) Effect of decontamination on the filtration efficiency of two filtering facepiece respirator models. J Int Soc Respir Protect; 24: 93–107.

Viscusi DJ, Bergman MS, Eimer BC, *et al*. (2009) Evaluation of five decontamination methods for filtering facepiece respirators. Ann Occup Hyg; 53: 815–27.

Viscusi DJ, Bergman MS, Novak DA, *et al*. (2011) Impact of three biological decontamination methods on filtering facepiece respirator fit, odor, comfort, and donning ease. J Occup Environ Hyg; 8: 426–36.

Vo E, Rengasamy S, Shaffer R. (2009) Development of a test system to evaluate procedures for decontamination of respirators containing viral droplets. Appl Environ Microbiol; 75: 7303–9.

Weber TP, Stilianakis NI. (2008) Inactivation of influenza A viruses in the environment and modes of transmission: a critical review. J Infect; 57: 361–73.

Woo IS, Rhee IK, Park HD. (2000) Differential damage in bacterial cells by microwave radiation on the basis of cell wall structure. Appl Environ Microbiol; 66: 2243–7.